Supplementary Materials for

Gating of Hippocampal Activity, Plasticity and Memory by Entorhinal Cortex Long-Range Inhibition

Jayeeta Basu[1*#], Jeffrey D. Zaremba[1^], Stephanie K. Cheung[1^ #], Frederick L. Hitti[1], Boris V. Zemelman[3], Attila Losonczy[1] and Steven A. Siegelbaum[1,2*]

*Correspondence to: JB, jayeeta.basu@nyumc.org and SAS, sas8@columbia.edu

^Equal contribution

This PDF file includes:

Other Supplementary Materials for this manuscript includes the following:

Methods

All experiments were conducted in accordance with the National Institutes of Health guidelines and with the approval of the Columbia University and New York State Psychiatry Institute (NYSPI) Institutional Animal Care and Use Committee.

Mice: Gad2-IRES-Cre (*16*), PV-IRES-Cre (*54*), and Ai14-tdTomato (*55*) mouse lines were obtained from the Jackson Laboratory (JAX). The CCK IN specific EGFP labeled line was generated as described in (*11, 16*). Briefly CCK-IRES-Cre driver (generous gift of Z.Josh Huang, Cold Spring Harbor Laboratory) (*16*); (*11*) mice were crossed with the Dlx5/6-Flpe driver mice (generous gift from Gord Fishell, New York University, (*56*)) and a Cre- and Flp-dependent EGFP reporter strain, R26NZG (JAX, (*57*)).

Viruses: Anatomy and slice electrophysiology experiments in Figure 1 utilized: 1) rAAV2/1 EF1α-DIO-ChR2-EYFP (Karl Deisseroth, Stanford University); 2) AAV2/9 CAG-Flex-EGFP; and 3) rAAV2/9 CAG-Flex-tdTomato, (all prepared by UPenn Vector Core). Behavior experiments in Figure 2 utilized: 1) For the PSAM silencing group rAAV2/9 Syn-Flex-PSAM(L141F)GlyR-IRES-GFP (plasmid generous gift from Scott Sternson, Janelia Farm; prepared by UPenn Vector Core); and 2) For the GFP Control group rAAV2/9 Syn-Flex-EGFP (Bryan Roth, University of North Carolina; prepared by UNC Vector Core). Imaging experiments in Fig. 3 utilized rAAV2/1 Syn-Flex-GCaMP6f (Loren Looger, Janelia

Farm; prepared by UPenn Vector Core). The following custom prepared viruses were used for the LRIP activation and silencing experiments in Figure 5 G-L, 5I-K and 6D-H: 1) rAAV2/7 Syn-Flex-Chr2-sfGFP; and 2) rAAV2/7 Syn-Flex-PSAM-IRES-GFP (Boris Zemelman, UT Austin, both custom prepared). Experiments in Fig. 6 A-E involving: 1) photostimulation of GABAergic CCK-Cre^{+} INs used an rAAV2/7 Gad65-(Chr2-sfGFP)^{Cre} (Boris Zemelman, UT Austin, custom prepared); 2) photostimulation of PV-Cre^{+} INs used rAAV 2/5 EF1α-DIO-ChR2-EYFP (Karl Deisseroth, Stanford University commercially derived from UPenn, (*58*)).

Surgery:

Stereotaxic virus injection. The viral injection procedure is as previously described (*11*), (*59*). Virus was injected into the brains of mice under stereotactic control using thin glass pipettes pulled using a micropipette puller and fire-polished using a microforge to have a long taper ending with a 10 μm tip diameter. Pipettes were first back-filled with light mineral oil, then front-filled with the virus using a Nanoject II injector. Adult mice (5-10 weeks old) were injected with 50 μL buprenorphine (0.3 mg/mL), subsequently anesthetized with 3.5% isofluorane for 3 mins (1.5 ml/mins flow rate) in an induction chamber, headfixed in a stereotaxic frame.and maintained under anesthesia with 1.5-2.5% isofluorane (1 ml/min) with a facemask. The hair on the head was clipped, the scalp sterilized with ethanol and betadine and a 5-7 mm incision made to expose the skull.

The skull was then cleaned with hydrogen peroxide (0.1%), and the level adjusted to align bregma and lambda in the z-axis. Small craniotomies were made bilaterally to target the dorsal hippocampal CA1 subfield (A/P, -2.3 ± 0.2 from Bregma; M/L, 1.5 ± 0.2 from Bregma, D/V, -1.2 ± 0.2 mm from surface of the brain), LEC (A/P, -3.2 ± 0.2 from Bregma; M/L, 4.5 ± 0.2 from Bregma, D/V, -2.5 ± 0.2 mm) and MEC (A/P 0.2 ± 0.2 from lamboid sinus at a 9° angle, M/L 3.1 ± 0.2 from lambda, D/V 0.9 ± 0.1 from surface of the brain). The pipette was lowered to penetrate the dura and a total of ~92-115 nl of virus was injected at each stereotactic coordinate (23 nl at a time with a 30-s interval between injections) using the Nanoject II auto injector under slow mode. The pipette was retracted from the brain after a 5 minute waiting period following the final injection per site. The scalp was disinfected with betadine, treated with triple antibiotic and the topical anesthetic Marcaine (0.5%), and sutured. Mice were allowed to recover for 2-4 weeks post injection before the electrophysiology experiments.

Hippocampal cannula guide implantation. To selectively silence the long-range inhibitory projections from the entorhinal cortex to the hippocampus we used local infusion of the cognate synthetic ligand PSEM in CA1 using a cannula. The pre-surgical and craniotomy procedures were identical to that of the stereotaxic viral injection. The skull surface was dried completely and coated with a thin layer of vetbond and then lightly scratched using a scalpel blade to form crevices for the cement mix to seep in. A sterilized custom designed bilateral cannula guide

with a dummy cannula was inserted in the skull over dorsal hippocampal CA1 (A/P, -2.2; M/L, 1.5, D/V, -1.7 from Bregma) along with two stainless steel anchoring screws inserted partially into the skull, one over the prefrontal cortex and the other over the cerebellum. The implant was secured to the animal's skull using dental cement (grip cement, or dental acrylic) and 2 bone screws. The cement was allowed to dry for 20 minutes and the wound sutured around the implant. Marcaine was applied locally to decrease postoperative pain.

Hippocampal cranial window implantation. The cranial window implantation method used here is as described previously (*27, 28*). The pre-surgical anesthesia and exposed skull preparation procedures were identical to that described above. A 3-mm diameter circle was drilled in the skull over left dorsal CA1, to match the size of the cannula window implant. The bone and dura were gently removed, and the cortex covering the hippocampus was slowly aspirated while constantly irrigating with chilled ACSF until the external capsule was exposed. A sterilized stainless steel cannula implant with a glass cover slip window was inserted into the craniotomy. The top of the cannula and a titanium headpost was secured to the skull with grip cement. The cement was allowed to dry for 20 min before returning mice to the home cage.

Post-surgical care. The animals recovered from anesthesia and were mobile within 5-15 mins post surgery. Mice were monitored every 12 hours for three

days after surgery, and buprenorphine was administered to minimize any signs of discomfort.

Freely moving behavior: The behavioral tests were performed as described previously (*20*).

Subjects and Habituation. 4-5 male mice were housed per cage with *ad lib* access to food and water, kept on a 12-h (6 a.m. to 6 p.m.) light–dark cycle with the ambient temperature maintained at 21°C. Tests were conducted during the light cycle. Half of the littermate mice in each cage were injected with the control GFP virus bilaterally in LEC, while the other half was injected with the PSAM virus. For 5 days prior to start of behavioral testing the mice were habituated to handling, transport from the post-procedural housing room to the behavioral testing room and momentary head restraint for connecting the cannula guide with dummy tubing. During these habituation sessions mice were allowed to move around with the tubing attached to simulate the PSEM infusion conditions. The experimenter was blind to the group identities, which were revealed after testing was completed.

Microinfusion of PSEM. An internal injection cannula was connected to a 10 μl Hamilton syringe via thin tubing. The tubing was pre-filled with steri-filtered PSEM 308 (15 μM) in oxygen enriched ACSF and the syringe was mounted in a syringe pump. The animal was gently restrained in its homecage by hand and the injection cannula was slowly introduced into the previously implanted guide

cannula. The cannula was fixed to the head implant via a screw-top connector, and the animal was released in an empty cage. Next 0.5 microliters of PSEM was injected over the course of 5 minutes using the syringe pump, followed by a 2 minute rest period with the tubing connected to the animal. The animal was gently restrained once again by hand, the connector detached, the internal cannula removed and the dummy internal cannula restored to the guide cannula. The animal was then placed in the open field, CFC chamber, or object recognition arena for testing in the behavioral tasks.

During all microinfusion experiments, the dye miniRuby (5% in water) was included in the cannula solution to gauge post hoc the accuracy of cannula targeting and spread of substances during the microinfusion. At the end of the experiments, the animals were infused with miniRuby again, 10 minutes prior to perfusion with PFA and the brains were examined for miniRuby fluorescence. These experiments provide an overestimate of the likely extent of PSEM diffusion during its application as the brains were analyzed 1 - 24 hrs after the first miniRuby infusion and subjected to more than one miniRuby infusions, whereas PSEM is only active for 20 minutes following application (*19*).

Open field. Mice were placed in an open field (45cm L x 45cm W x 30.5cm) for 30 minutes. The testing chambers were cleaned with 70% isopropanol wipes between animals to eliminate any odor related cues. Locomotor and rearing activity was monitored via motion sensitive IR beam breaks and recorded by the

Activity Monitor software. The entire apparatus was enclosed in a sound proof box.

Contextual and Cued Fear Conditioning. Hippocampal-dependent contextual fear memory and amygdala-dependent auditory fear memory was tested using a 3-day delay fear conditioning protocol. A sound-attenuating chamber equipped with a FireWire camera for tracking, a light, and a speaker for delivering contextual and conditioning cues was used. Mice were placed in an enclosure (17cm x 17cm x 25cm) housed within the sound-attenuated chamber. The flooring, wall patterns, dominant odors, and light conditions of the enclosure could be changed to provide different contexts. Context A on Day 1 consisted of an enclosure with a steel grid floor, 3 plexiglass walls and 1 opaque wall with black and white stripes, 1% acetic acid as the dominant odor, and the house fan turned on. The enclosure was cleaned with 70% isopropanol between animals. Mice were moved from their home cage to a transfer cage with no bedding for the PSEM microinfusion as detailed above. Two minutes post-infusion of PSEM, the mice were placed in the fear conditioning chamber (context A). The mice explored the environment for 150 s, following which a tone (30 s, 2.8 kHz, 85 dB) was presented that co-terminated with a shock (2 s, 0.7 mA). Mice were removed from the chamber 30 s following the shock. On Day 2, the mice were placed back in context A for 300 s and contextual fear memory was assayed by scoring percent time spent freezing (defined as the absence of all movement except for respiration). No shock or tone was presented on Day 2.

On Day 3, the mice were exposed to novel context B: the testing room was dimly illuminated with red light and the enclosure was cleaned between animals with Vimoba; the enclosure had an opaque white colored plastic floor, with 3 solid gray colored walls, 1 plexiglass wall with a circular door, and a red, flat plastic roof and 0.25% benzaldehyde as the dominant odor. Mice were first moved from their home cage to a circular bucket and then a cage with paper towel bedding during PSEM infusion before moving them to the testing chamber. Mice were exposed to context B for 180 s, and then the tone from day 1 was played for 60 s to assess cued fear conditioning using percent time spent freezing. Freezing during fear conditioning was analyzed automated with ANY-maze and parsed into the different behavioral task phases.

Novel Object Recognition (NOR). Twelve male mice were injected with AAV9-Syn-FLEX-PSAM L141F:GlyR-IRES-GFP (Penn) and kept on a 12h reversed light-dark cycle in a room maintained at 21 °C. All trials of the novel object recognition task were conducted during the dark cycle and in dim lighting. White plastic transport boxes (55 x 40 x 15 cm^3) were used as testing arenas. Three different objects were used: (1) a blue ceramic shoe (diameter 9.5 cm, maximal height 6 cm), (2) a black plastic slidebox (8 x 3 x 9.5 cm^3), and (3) a semi-clear plastic funnel (diameter 8.5 cm, maximal height 8.5 cm). In pilot experiments, we found these objects elicited equal exploration time. Mice were habituated to handling and transported from the holding room to the behavioral room and were given 1 hour in behavioral room each day to habituate before any tasks began.

Mice were habituated to the infusion set-up and empty testing arena for 10 minutes each day for three consecutive days. On the fourth day, mice were infused over a duration of 5 minutes with either miniRuby + ACSF + PSEM or a control solution of miniRuby + ACSF. The solutions were kept in coded tubes to ensure that the experimenter was blinded and to randomize the treatment groups. In trial 1, mice were exposed to object A and object B for 10 minutes. Following a 3 minute inter-trial interval, mice were again exposed to the same pair of objects for trial 2. The mice were then tested for object recognition memory after a 10 minute interval by replacing either object A or object B with object C, the novel object. We adopted our NOR task based on the study by Denny et al. (*25*), but increased the inter-trial interval to 10 minutes to ensure that it would be dependent on hippocampus *(20-23)*. Objects and arenas were cleaned with 30% ethanol between all trials. Mice were recorded with an overhead FireWire camera and their movements tracked using ANY-maze software. Exploration time was determined using ANY-maze by measuring time spent with the animal's head within a region-of-interest (ROI) that extended 2 cm around each object.

***In vivo* imaging with head-fixed behavioral cues:** Imaging experiments in headfixed, awake behaving mice were performed as described previously(*27*)' (*28*). Briefly, Gad2-Cre: Ai14 tdTomato mice were injected in the left LEC with Cre-dependent rAAV to express the genetically encoded calcium indicator

GCaMP6f (*26*) selectively in Cre^+ GABAergic neurons within the LEC. Two weeks post-injection, a glass-bottomed stainless steel cannula was implanted directly over the left hippocampus to allow for optical access to the long-range GABAergic axons projecting from LEC to SLM. After 1 week of recovery, water-deprived mice were head-fixed on a treadmill belt under a two-photon laser-scanning microscope within a custom-built behavioral apparatus that allows for simultaneous imaging and recording of behavior in response to four sensory stimuli: an aversive airpuff to the snout, an appetitive water reward, a flash of light, and pure tones. Each experiment contained 3-5 blocks of stimuli presented either singularly or in pairs. Locomotion was monitored while imaging during each trial, which consisted of a 5-10 second pre-trial interval, a randomly chosen stimulus or pair of stimuli, and a 10-30 second post-trial recording interval. Imaging was performed with an ultra-fast pulsed laser beam (920-nm wavelength; 20–40 mW average power at the back focal plane of the objective) through a 40X objective. Green (GCaMP) and red (tdTomato) fluorescence was separated with an emission filter cube set (green, HQ525/70m-2p; red, HQ607/45m-2p; 575dcxr) and was detected with photomultiplier tubes (green: GaAsP PMT; red: multi-alkali PMT) at either 256 X 128 pixels (75 x 75 μm; 0.295 *μ*m/pixel in X; 0.588*μ*m/pixel in Y), 4x optical zoom, at 5.3 Hz or 128 x 128 pixels (105 x 105 μm), 2.8x optical zoon, at 6.1 Hz.

Acute Slice Electrophysiology:

Solutions. Recordings were performed using artificial cerebrospinal fluid (ACSF, pH 7.3, osmolarity 305-320 mOsm and saturated with 95% O_2 and 5% CO_2) for the extracellular solution. The ACSF consisted of (in mM): NaCl (125), $NaHCO_3$ (25), KCl (2.5), NaH_2PO_4 (1.25), $MgCl_2$ (1), $CaCl_2$ (2), glucose (22.5), Na-pyruvate (3), ascorbate (1). Hippocampal slices were prepared and incubated in sucrose-enriched modified ACSF containing (in mM): NaCl (10), NaH_2PO_4 (1.2), KCl (2.5), $NaHCO_3$ (25), glucose (25), $CaCl_2$ (0.5), $MgCl_2$ (7), sucrose (190), pyruvate (2). The intracellular current-clamp recording solution contained (in mM): $KMeSO_4$ (135), KCl (5), NaCl (2), EGTA (0.2), HEPES (10), phosphocreatineNa_2 (10), MgATP (5), Na_2GTP (0.4), Alexa Fluor 594 cadaverine (0.1) and Biocytin (0.2%). The intracellular solution for voltage-clamp recordings contained: $CsMeSO_4$ (135), KCl (5), NaCl (2), EGTA (0.2), HEPES (10), phosphocreatineNa_2 (10), MgATP (5), Na_2GTP (0.4), Alexa Fluor 594 (0.1) and Biocytin (0.2%). In a subset of experiments, the following drugs were applied via bath application (in μM): SR95531 (2), CGP55845 (1), NBQX (10), D-APV (100), PSEM^{308} (3-5). PSEMwas generously provided by Dr. Scott Sternson, Janelia Farm.

Slice Preparation. We prepared 400-μm thick horizontal hippocampal sections using a vibrating microtome from brains of mice that were transcardially perfused with ice-cold dissection ACSF. For the horizontal sections, hemisected brains were blocked ventro-medially at an angle of 10^o before sectioning. For the transverse sections, the hippocampi were dissected out, embedded in agar (4%)

and then sliced. Slices were allowed to recover for at least 20 mins at 34^{o}C and then stored at room temperature in a 50% dissection: 50% standard ACSF solution before transfer to the recording chamber.

Electrophysiology setup. For infrared- (IR) guided patch recordings, slices were visualized with a microscope equipped with Dodt Gradient Contrast optics and a 2-4X zoom module, IR filter, 60X 1.0 nA water immersion objective and a camera using image acquisition software. We performed fluorescence-guided targeted patch clamp recordings using an epifluorescence illumination system equipped with a metal-halide lamp, ET-GFP and mCherry filter sets, Uniblitz shutter VCM-D1, and Orca R2 CCD camera controlled by *μ*-Manager. Photostimulation of ChR2 was achieved with an optical fiber coupled to a solid state blue laser (470 nm) to illuminate SLM. In some experiments the light was routed through a set of pinholes to produce a 50 *μ*m focal beam spot over SR.

Two-photon imaging and electrophysiology setup. Two photon imaging of proximal dendritic spine Ca^{2+} used a custom-designed system with dual X-Y scanning galvanometers, coupled to a pulsed Ti:Sapphire MaiTai DeepSee femtosecond laser. Fluorescence was detected using high-sensitivity GaAsP photomultiplier tubes. The scanning system was mounted on a microscope, equipped with a 60X 0.9 NA water immersion objective, and infrared Dodt Gradient Contrast optics coupled to a multi-alkali detector. Recording and stimulating electrodes were positioned using three junior micromanipulators on a movable motorized base plate connected to a multiclamp 700B amplifier,

Digidata 1440, and two constant-current stimulators for patch clamp electrophysiology during imaging.

Electrophysiology recordings. Whole cell patch clamp recordings were performed at 34^{o}C in standard ACSF using borosilicate glass pipettes with tip resistances of 3.5-4.5 MΩ for somatic and 9-16 MΩ for dendritic recordings. A Multiclamp 700B Amplifier, pClamp 9 software and a PC were used for data acquisition. Pipette capacitance (Cp), series resistance (Rs) and whole cell capacitance (Cm) were compensated under voltage clamp initially with maximal allowable prediction and correction (75-85%). The average series resistance for whole cell voltage-clamp recordings was kept between 9-15 MΩ. These values were used as a guide to estimate the pipette capacitance compensation and bridge balance under current clamp. The average access resistances for the current clamp recordings ranged from 10-20 MΩ for soma and 10-40 MΩ for dendrite recordings. The membrane potential (V_m) of IN and PN soma were held at +10 mV under voltage clamp to measure IPSCs, while current clamp recordings were performed from soma and dendrites at the cell's resting membrane potential.

Synaptic responses were evoked by electrical stimulation of the entorhinal cortex (EC) inputs or Schaffer collaterals (SC), using focal glass pipette stimulating electrodes coupled to constant current stimulators placed in stratum lacunosum moleculare (SLM) or stratum radiatum (SR), respectively. Stimulus strengths were adjusted to evoke EC and SC PSPs <50% of their maximal amplitude. Basal transmission was monitored every 15 s with EC and SC

electrical stimuli spaced 2 s apart**.** Laser pulses delivered during episodes involving optical stimulation were also spaced 15 s apart. Cells were intracellularly filled for 10-15 minutes with the Ca^{2+} indicator Fluo-5F (500μM) and the structural dye Alexa fluor 594 (25 μM). Random access line scans (256 lines per frame, 5.6X optical zoom, 25.709 x 17.504 μm FOV, 2.8 μs dwell time, 1.28 ms scanline period) and 2-D scan (512 X 512 pixels, 1X optical zoom, 198.45 x 198.45 μm FOV, 1.6 μs dwell time, 1.4 ms scanline period) image series were acquired using the PrairieView software in both the green and red channel. The image t-series acquisition on PrairieView was synched and TTL triggered by the electrophysiology acquisition software Axograph. Line scans were acquired after each EC-SC stimulus pair simultaneously with the SC stimulus trigger once every 15 s for the single pairings at variable timing intervals (0-40 ms). For multiple pairings at 10 or 20 ms intervals, images were acquired at a 1 Hz frequency up to 90 times, identical to the ITDP induction protocol.

Immunohistochemistry, Confocal Imaging and Neuronal Tracing:

Immunohistochemistry- Adult animals were deeply anesthetized with Ketamine/Xylazine, and perfused with 1X PBS followed by 4% paraformaldehyde in PBS. The brains were removed and post-fixed overnight in 4% paraformaldehyde at 4°C. The brains were sectioned in the coronal plane for hippocampal sections or sagittal plane for entorhinal sections at 50 μm thickness using a vibrating microtome. For experiments involving the expression of GFP

alone, GCaMP and TdTomato, the signal was bright enough and did not require further immuno-enhancement. For immunostaining slices were permeabilized in 1X PBS + 0.3% triton, blocked in 3% Normal goat serum, and then incubated with primary (overnight) and secondary (2-4 hours) antibodies in blocking solution (1X PBS, 0.2% triton and 3% NGS), unless otherwise stated. ChR2-EYFP and ChR2-GFP-labeled neurons and their projections were stained using a rabbit polyclonal anti-GFP primary antibody (1:1000; Invitrogen) with a goat anti-rabbit Alexa Fluor 488 dye-conjugated IgG antibody (1:1000; Invitrogen). For the GFP-tagged CCK, PV and SOM interneuron triple staining, we used a similar procedure for washing, permeabilization and blocking as described above but substituted PBS with Tris-buffer solution (TBS, TB 0.1M; NaCl 0.9%; pH7.4). The primary antibodies we used were chicken polyclonal anti-GFP (1: 1000, abcam), rabbit polyclonal anti-parvalbumin (1:500, SynapticSystems/SYSY) and rat monoclonal anti-somatostatin (1:200, Millipore, clone YC7). The secondary antibodies for these stains included goat anti-chicken Alexa Fluor 488 dye-conjugated IgG (1:1000, Invitrogen), goat anti-rabbit Alexa Fluor 555 dye-conjugated IgG (1:1000, Invitrogen) and minimal cross reactivity goat anti-rat Alexa Fluor 647 dye-conjugated IgG (1:1000, Jackson Laboratories).

For experiments involving PSAM and CCK following electrophysiology recordings, 400 μm slices were drop-fixed overnight in 4% PFA, embedded in agar, and resectioned to 50 μm. For the α-bungarotoxin staining of PSAM-GlyR, we

followed the procedure previously described (*11*). Resliced sections were permeabilized with 0.5% Triton using a Tris-buffered saline (TBS) at a pH of 7.4. The slices were blocked in 10% Normal Goat Serum in TBS with 0.5% Triton for four hours at room temperature and then incubated with Alexa Fluor 647 α-bungarotoxin (1:3000; Invitrogen) in TBS + 0.1% Triton, first at room temperature for one hour, then at 4°C for 48 hours to stain for nicotinic α7 receptor-containing $PSAM^{L141F}$-GlyR. In sections that coexpressed ChR2-GFP or GFP alone with the PSAM, primary antibody for GFP (rabbit polyclonal anti-GFP primary antibody, 1:1000; Invitrogen) was added for the last 12 hours of overnight incubation at 4 °C. Following TBS washes (4x15 mins), the slices were incubated at room temperature for 4 hours with secondary antibody for GFP (goat anti-rabbit Alexa Fluor 488, 1:1000; Invitrogen) along with fresh Alexa Fluor 647 α-bungarotoxin (1:3000; Invitrogen) in TBS + 0.1% Triton to counterstain for GFP and PSAM . For the CCK staining, we followed a previously described procedure (*60*).

Briefly, slices were put through antigen retrieval by being placed in a citrate buffer at pH 8.6 for 70 minutes at 90°C. Then, slices were washed three times for five minutes each time in PBS. Slices were permeablized with blocking solution (1% BSA and 0.5% Triton in PBS) with 10% Normal Goat Serum for four hours at room temperature. Slices were then incubated with primary antibodies against cholecystokinin (mouse monoclonal; 1:1000; generous gift of Dr. Ohning, CURE center, UCLA) or GFP (rabbit polyclonal; 1:1000; Invitrogen) in blocking solution for 48 hours at 4°C. Slices were then washed four times for fifteen

minutes each time with carrier solution (1% BSA, 0.1% Triton, and 1% Normal Goat Serum in PBS) at room temperature. Following this, slices were incubated with a Biotin-SP-conjugated AffiniPure F(ab')$_2$ Fragment Goat anti-Mouse IgG (1:250; Jackson) and goat anti-rabbit Alexa Fluor 488 dye-conjugated IgG antibody (1:1000; Invitrogen) in carrier solution for four hours at room temperature. Following PBS washes (4 X 15 minutes), the slices were incubated in ABC complex for one hour. Then slices were washed with PBS (4 X 15 minutes) and incubated with TSA-tyramide-tetramethylrhodamine amplification kit plus buffer solution for 3-10 minutes at room temperature. PBS washed slices were next incubated with Alexa Fluor 555 Streptavidin (1:500; Invitrogen), Alexa Fluor 488 dye-conjugated anti-rabbit IgG secondary antibody (1:1000; Invitrogen), and Alexa Fluor 555 dye-conjugated anti-mouse IgG secondary antibody (1:1000; Invitrogen) in carrier solution for four hours at room temperature. Finally the slices were washed in PBS (4 X 15 minutes) and mounted.

Stained slices were mounted with Prolong Gold or Vectashield Hard Set Mounting Medium with DAPI for the GFP, CCK, PV and SOM stains or Aqua-Mount Aqueous Mounting Medium for the bungarotoxin staining.

Confocal Imaging. An inverted laser scanning confocal microscope was used to acquire tile scan and Z-stack images of multichannel fluorescent signals from fixed tissue sections using 5X, 10X or 20X air objectives as well as a high NA

63X oil immersion objective. Maximum intensity projections were created using ImageJ.

Neuronal Reconstruction. During the electrophysiology recordings all cells were intracellularly filled with Alexa fluor 594 for online visualization and 0.2% neurobiotin to allow for enhanced visualization and post-hoc reconstruction with a streptavidin-bound fluorophore (Streptavidin Alexa Fluor 555). Immediately after recording, the acute brain slice was drop fixed overnight at 4°C in 4% paraformaldehyde solution. The tissue was then thoroughly rinsed with PBS-Glycine (1 X 15 min) and PBS (3 X 15 min) and processed for immunohistochemistry. The 20X high resolution (1024X1024, 16 bit depth) fluorescent confocal Z-stack images of the fluorophore-labeled filled neurons were used to trace the soma, axons and dendrites using Neurolucida reconstruction software.

Data Analysis

Behavior data. For the behavioral experiments the open field data was analyzed using Activity Monitor and an automated analysis was used for calculating freezing during fear conditioning with ANY-maze. The data were exported in tab-delimited format into Prism for further statistical analysis. The red fluorescent signal of miniRuby infused along with PSEM during the behavioral tasks served as an indicator of accurate cannula targeting and drug spread. One animal from

the control cohort (total of 10 animals) and test cohort (total of 8 animals) each was removed from the data analysis due to mistargeting. Statistical significance was assessed by two-tailed unpaired Student's t-tests, 2-way ANOVA, or 2-way repeated measures ANOVA where appropriate. Significant main effects or interactions were followed up with multiple comparison testing using Sidak's correction. Results were considered significant when $P < 0.05$. α was set equal to 0.05 for multiple comparison tests. Sample sizes were chosen based on previous studies.

In vivo imaging data. 'Sequential Image Analysis (SIMA)' toolkit (*61*) was used to correct motion artifacts in the raw imaging data, identify and tag regions of interest (ROIs), and extract fluorescence traces from each ROI. Extracted signals were synchronized to the recorded running signal and presented stimuli, and peri-stimulus time-histograms (PSTHs) were calculated. For each ROI-stimulus pair, the response magnitude was calculated as the mean of the PSTH in the 3 seconds preceding the stimulus subtracted from the mean of the 3 seconds following the stimulus. Significantly responding ROIs were determined by randomly shuffling the stimulus times across all trials 10,000 times, calculating the response magnitude for each shuffle, and then selecting any ROIs with a response magnitude above the 95^{th} percentile of the distribution of shuffled values.

Electrophysiology data. Axograph X was used for electrophysiology data analysis. A 7 pA amplitude threshold was set for sorting failures and successes for the light evoked IPSCs to map the LEC and MEC LRIP connectivity. All IPSCs above this cutoff were included in calculating the mean response amplitude and % of responsive INs for the two groups. For calculating amplitude changes in the EC-SC and EC-ChR2 single pairing, the responses to SC electrical stimulation or ChR2 photostimulation alone were averaged for 3 minutes prior to pairing and the mean was used to normalize the responses paired with EC stimulation. For comparing the effect of application of NBQX, AP-V, SR, CGP or PSEM: the pre-drug baseline synaptic response amplitude for the 'control' condition was obtained by averaging the responses recorded for the 5 minutes preceding drug application. The post drug synaptic response amplitude were obtained by averaging responses recorded for 5 minutes in the presence of the drug, once a steady state response was reached, typically 7-10 minutes after starting bath application of the drug . For sorting and generating the histograms of the dendritic PSPs and spikes, an event detection algorithm in Axograph was used. Time course plots for ITDP were generated using a box-car average of every 4 responses (1 minute period) as previously described (*11*). All statistical errors are standard errors of the population mean or boxcar mean (SEM); all p values (significance level set at $P < 0.05$) for t-tests are two tailed and all ANOVAs were corrected for multiple comparisons using post-hoc tests as indicated.

Kaleidagraph 4 and Prism 6 were used for plotting all data and statistical analysis. Figures were generated with Adobe Illustrator.

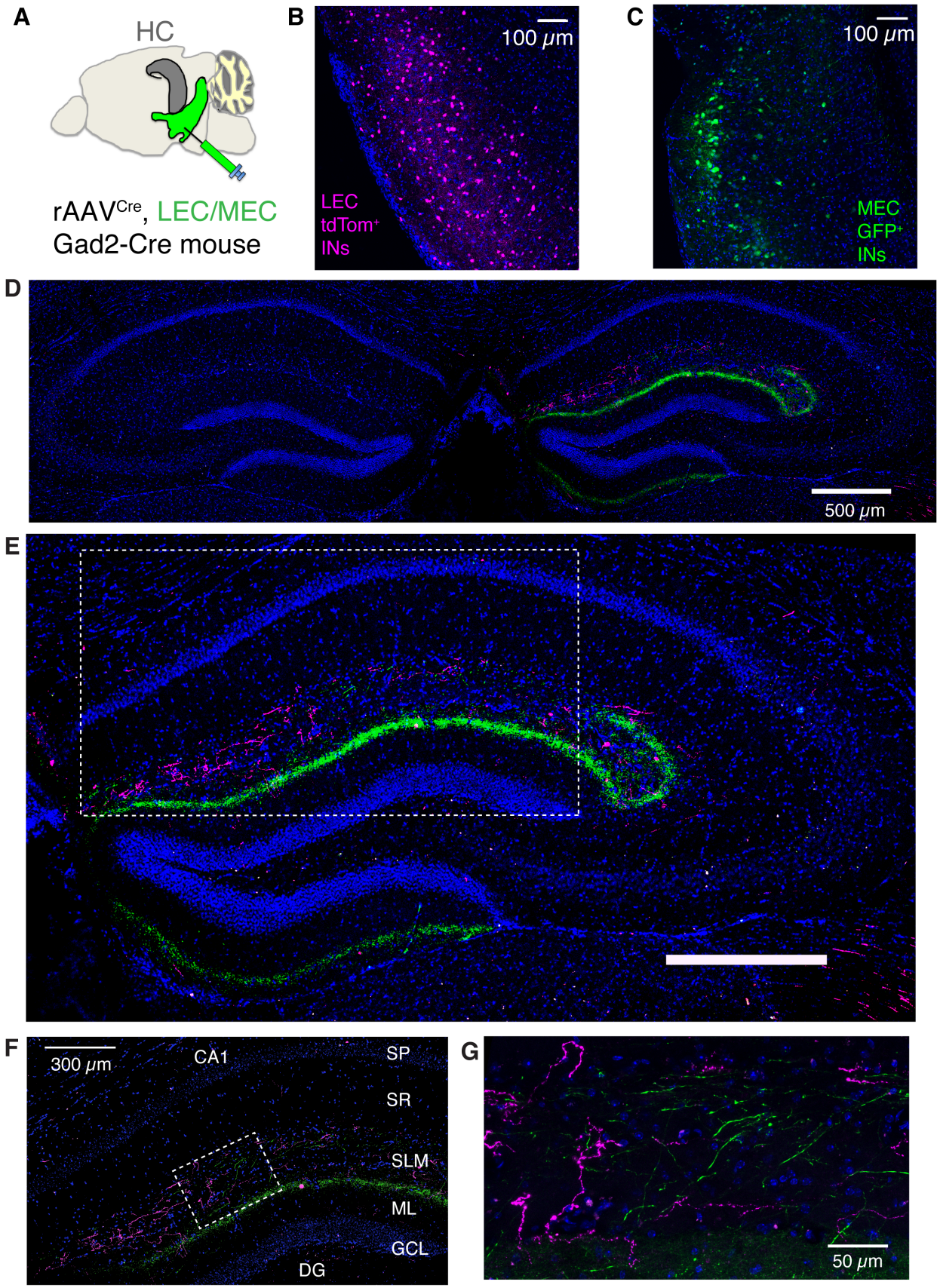
A
HC
rAAVCre, LEC/MEC
Gad2-Cre mouse
B
100 μm
LEC
tdTom+
INs
C
100 μm
MEC
GFP+
INs
D
500 μm
E
F
300 μm
CA1
SP
SR
SLM
ML
GCL
DG
G
50 μm

Fig. S1. LEC and MEC GABAergic projections in hippocampus. A. LEC and MEC viral injection sites (in green) and their hippocampal projections (HC, in grey). **B, C.** Images of injection sites showing AAV^{Cre} mediated expression of tdTomato (magenta) in LEC **(B)** and GFP (green) in MEC **(C)**. **D.**10X confocal image of a coronal section of right and left hemisphere hippocampi showing ipsilateral expression of tdTomato (magenta) and GFP (green) labeled GABAergic projection axons, following unilateral viral injections in LEC and MEC, respectively. **E.** 20X confocal projection image showing detailed expression pattern of LEC and MEC LRIPs in hippocampus from injected hemisphere. Note the greater expression of $tdTomato^{+}$ LEC LRIPs in SLM of CA1 compared to GFP^{+} MEC LRIPs, which tend to innervate the outer layer of DG. **F.** Zoomed in view of inset in E showing TdTomato- and GFP-labeled axons in SLM of CA1 from LEC and MEC Gad2-Cre^{+} LRIPs. DAPI stain in blue. **G.** 63X zoomed in view of inset in F.

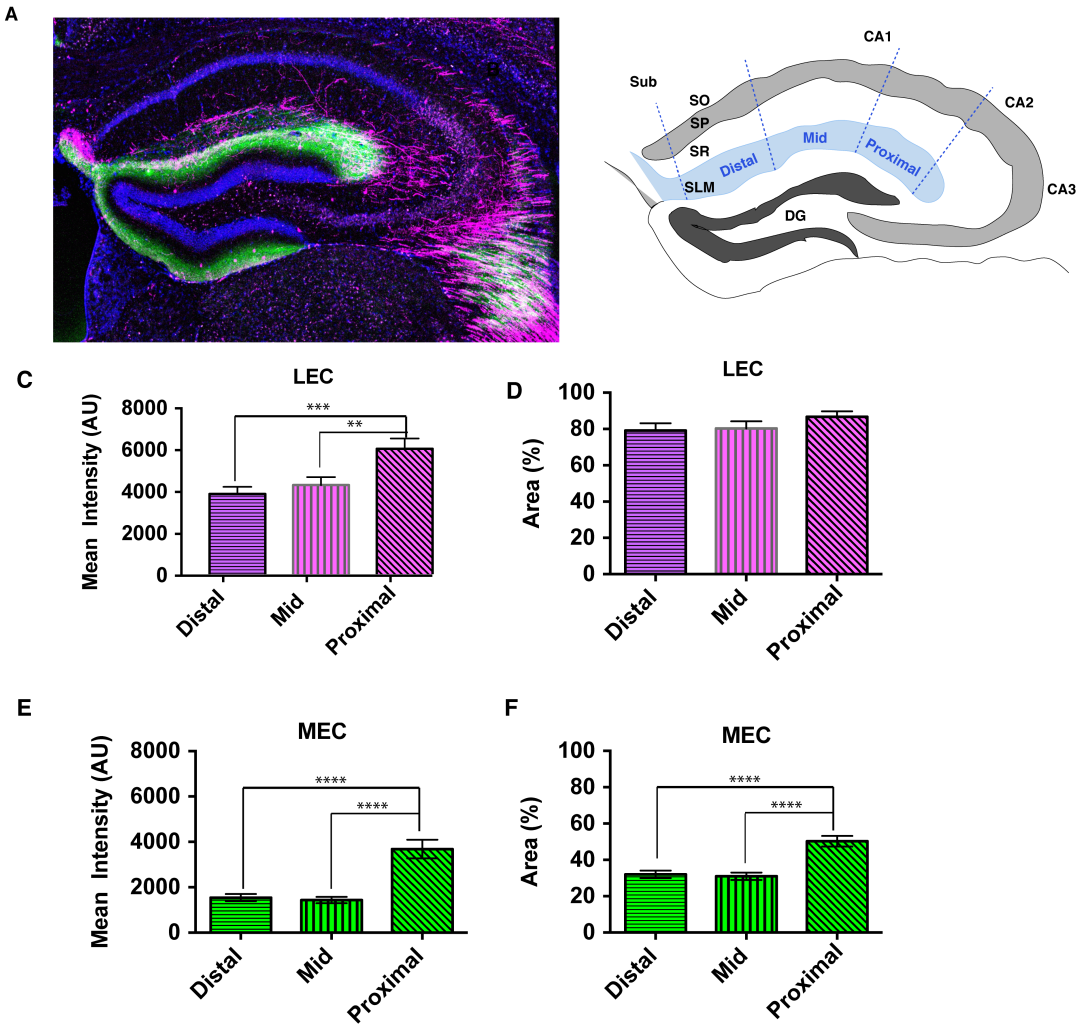

Fig. S2. LEC and MEC GABAergic projection pattern in CA1. A. 20X confocal projection image showing LRIPs from LEC (labeled with tdTomato, in magenta) and MEC (labeled with GFP, green) in the hippocampus from the injected hemisphere of a GAD2-Cre mouse injected with AAV^{Cre} expressing tdTomato in LEC and GFP in MEC. **B.** Schematic of hippocampus with the demarcation of the subfields (subiculum, sub; CA1; CA2; CA3, dentate gyrus-DG), layers (stratum oriens, SO; stratum pyramidale, SP; stratum radiatum, SR and stratum

lacunosum moleculare, SLM), and the division along the transverse axis into proximal (CA2 side of CA1), medial (mid CA1) and distal (subicular side of CA1) regions. Bar plots (Mean ± SEM) quantifying the fluorescence (mean intensity, AU) and spread (% area) of LRIP axons in CA1 originating from LEC (C-E, magenta) and MEC (F-H, green) in the proximal, medial and distal subdivisions of SLM in CA1. LRIP input from LEC to all regions of CA1 is significantly greater than LRIP input from MEC (using two-tailed t-tests), based on higher higher fluorescence intensity (Proximal CA1: LEC = 5991 ± 489.3 AU versus MEC = 3686 ± 412.2 AU; $P = 0.0005$; Mid CA1: LEC = 4258 ± 375.7 AU versus MEC = 1436 ± 141.6 AU; $P < 0.0001$; Distal CA1: LEC = 3829 ± 340.4 versus MEC = 1546 ± 158.8 AU, $P < 0.0001$). LEC LRIPs also covered a larger area of SLM in CA1 compared to MEC LRIPs (LEC = 82.05 ± 3.64 % of SLM versus MEC = 37.79 ± 2.35% of SLM; $P < 0.0001$). LEC LRIPs showed a small but significant preference to innervate SLM in proximal versus distal CA1 (Area: Distal = 79.15 ± 3.98% versus Proximal = 86.68 ± 3.04%; paired t-test $P < 0.007$). In contrast, MEC LRIPs targeted SLM of proximal CA1 to a greater extent than distal CA1 (proximal = 50.31 ± 2.92% versus distal = 32.04 ± 2.09%; paired t-test $P < 0.0001$).

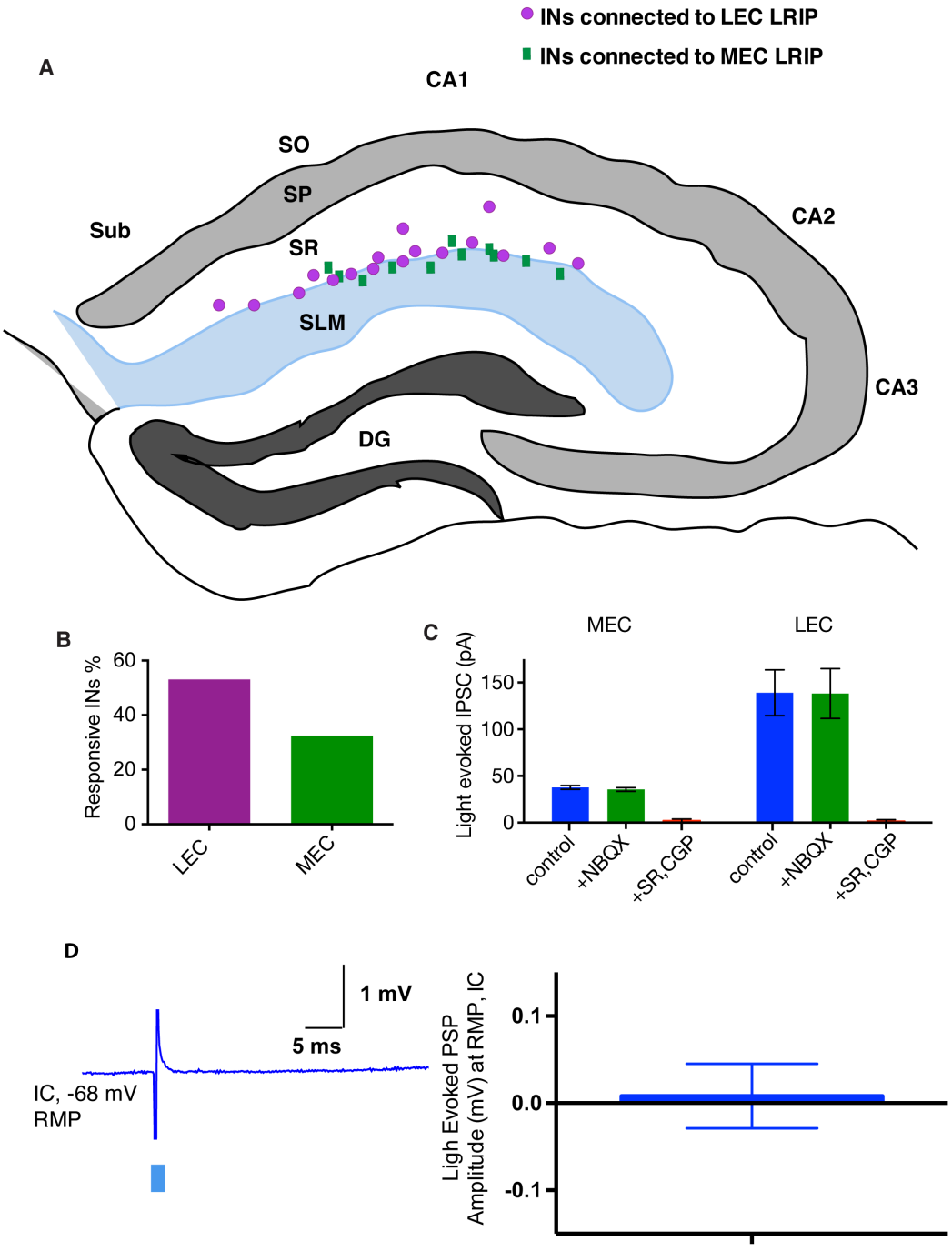

Fig. S3. LEC and MEC LRIP connectivity in SLM of CA1. A. Location of the cell bodies of the intracellularly recorded INs at the border of SR/SLM that responded to photostimulation of ChR2^{+} LRIPs from LEC (magenta circles) and

MEC (green rectangles). **B.** Percentage (%) of intracellularly recorded INs with cell bodies located in the border of SR/SLM of CA1 in which local photostimulation of ChR2$^+$ LRIPs from LEC (53.1% of neurons) versus MEC (32.4% of neurons) produced a light-evoked IPSC. The threshold for a response was set at an IPSC peak amplitude of ≥ 10 pA and a response probability of ≥ 50% per photostimulation episode at 100% laser power. **C.** Light-evoked IPSC amplitude (pA, mean ± SEM) recorded from CA1 SR/SLM border INs in response to photostimulation of ChR2$^+$ LRIP axons from either MEC or LEC under control conditions (drug-free ACSF, blue; MEC response = 37.74 ± 2.02 pA; LEC response = 139.00 ± 24.5 pA) or in the presence of 10 μM NBQX (green; MEC response = 35.5 ± 1.91 pA; P = 0.343 for control versus NBQX, paired t-test, n = 10; LEC response = 138.22 ± 26.7 pA, P = 0.286 for control versus NBQX, paired t-test, n = 15) and GABAR blockers (SR 2 μM, CGP 1 μM, red stripes; MEC response = 2.09 ± 1.78 pA, P < 0.0001, control versus SR, CGP; LEC response = 1.5 ± 1.69 pA, P < 0.0001, control versus. SR, CGP). Note that there is no significant difference between the control and NBQX groups whereas the IPSCs are eliminated upon GABAR blockade, confirming that the LRIPs provide direct GABAergic inputs from MEC and LEC. **D.** Example trace (left) and mean (± SEM) of light-evoked peak depolarizing PSP amplitude (mV) recorded from CA1 SR/SLM border INs under current clamp conditions at -68 mV in response to photostimulation of ChR2$^+$ LRIP axons from LEC.

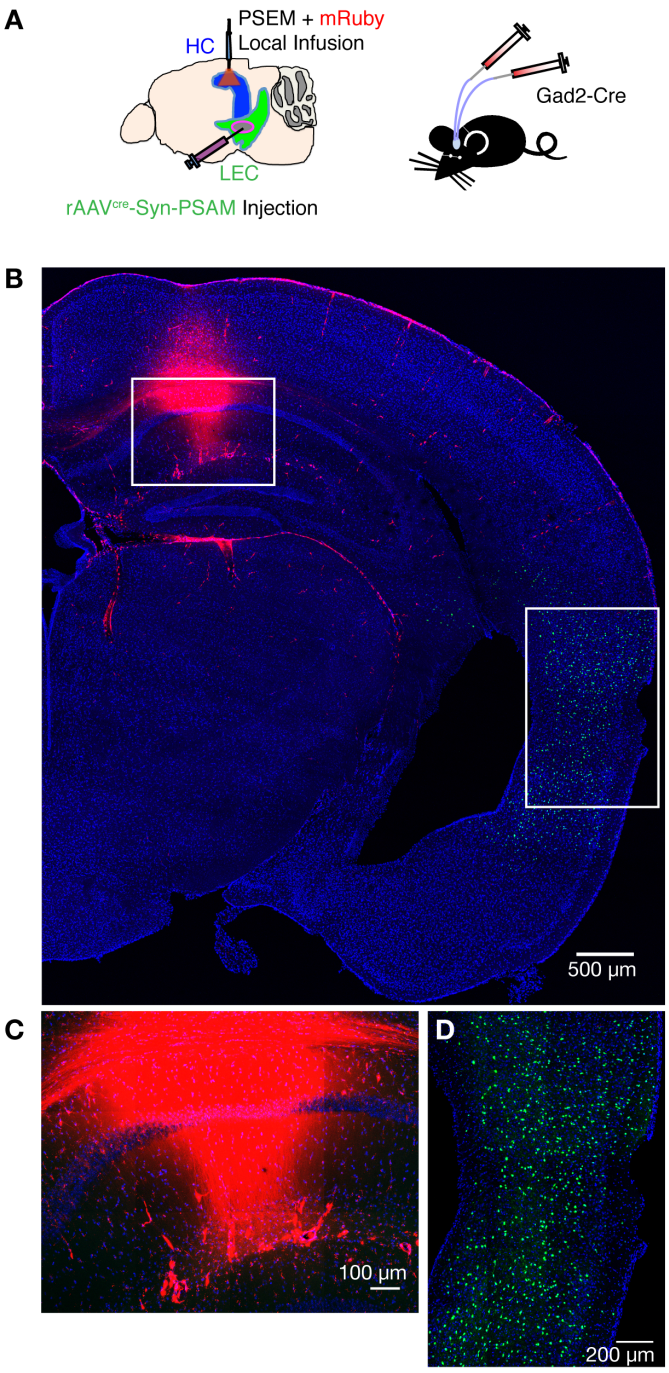

Fig. S4. Localization of PSEM and miniRuby to CA1 infusion site in Gad2Cre behavior cohorts. A. Diagram of the experimental design. Gad2-Cre mice were injected with AAV^{Cre} to express GFP or PSAM in LEC. An 0.5 µl

volume of PSEM 308 (15 μM) and miniRuby (5% in water) in ACSF was infused into the CA1 region of the hippocampus through a cannula. **B.** Example confocal image at 5X magnification of a coronal section derived from a Gad2-cre mouse used for behavioral testing that had been injected in LEC with an AAV^{Cre} expressing PSAM-2A-GFP. After infusion of PSEM and miniRuby solution, the mouse was sacrificed, approximately 10 min after the end of the infusion period. Image shows mini Ruby (red), DAPI (blue), and the expression of GFP in LEC (green). C. Higher magnification image showing miniRuby in CA1 restricted to a 1000 μm perimeter spanning the alveus, SO, SP, SR and SLM. **D.** Image showing absence of detectable miniRuby in LEC, which is positive for GFP (green) and DAPI (blue). The spread of miniRuby provides a likely upper limit of diffusion during the time course of the experiment as PSEM is rapidly metabolized, with an effect limited to 20 min after application (Personal communication S.Sternson; (*22*)). In contrast, miniRuby was able to diffuse for 72 hours between time of infusion and brain fixation.

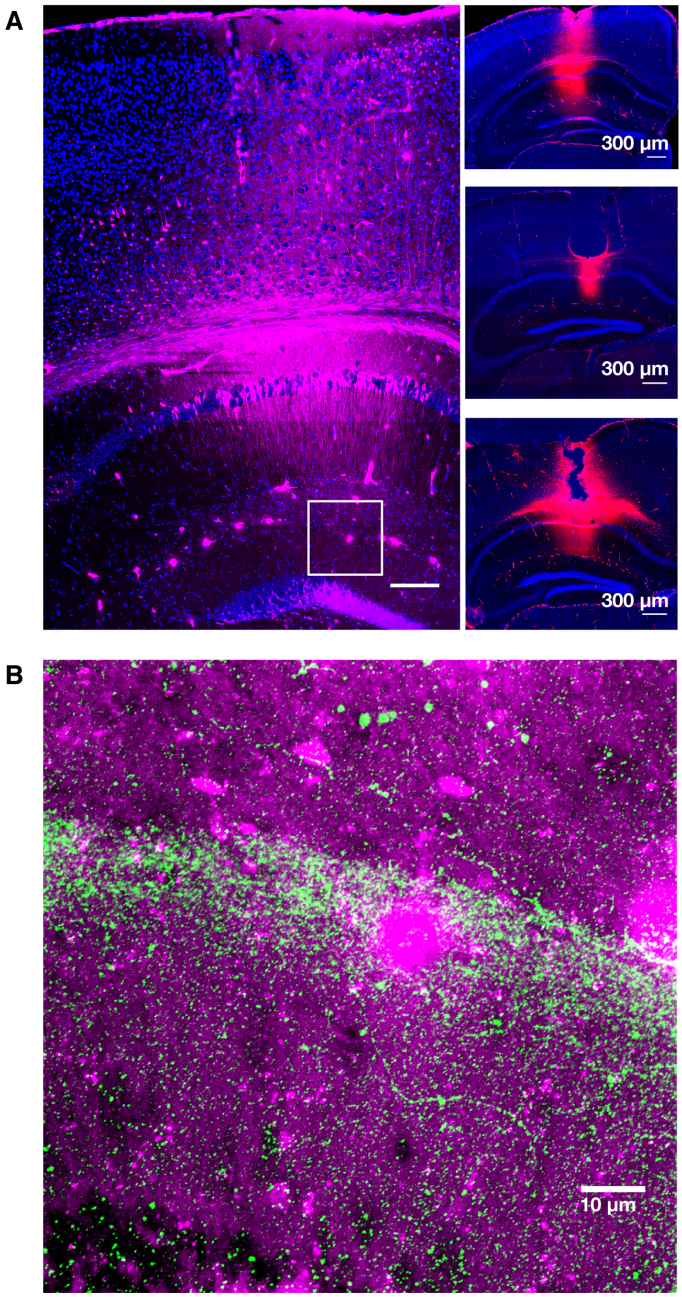

Fig S5. Additional Examples of Localization of PSEM and MiniRuby to CA1 infusion site in Gad2Cre Behavior Cohort. A. Additional confocal images taken at 20x (image on left) and 5X (images on right) magnification of coronal

sections derived from Gad2-cre mice used for behavioral testing that had been injected in LEC with an AAV^{Cre} expressing PSAM-2A-GFP. The mice received an infusion of PSEM and miniRuby solution and were sacrificed approximately 10 min after the end of the 5 min infusion period. Images show miniRuby (magenta in image on left, red in images on right) and DAPI (blue). **B.** Zoomed in image of left image of A, showing miniRuby (magenta) overlap of GFP (green) expressing fibers in SLM/SR border of CA1.

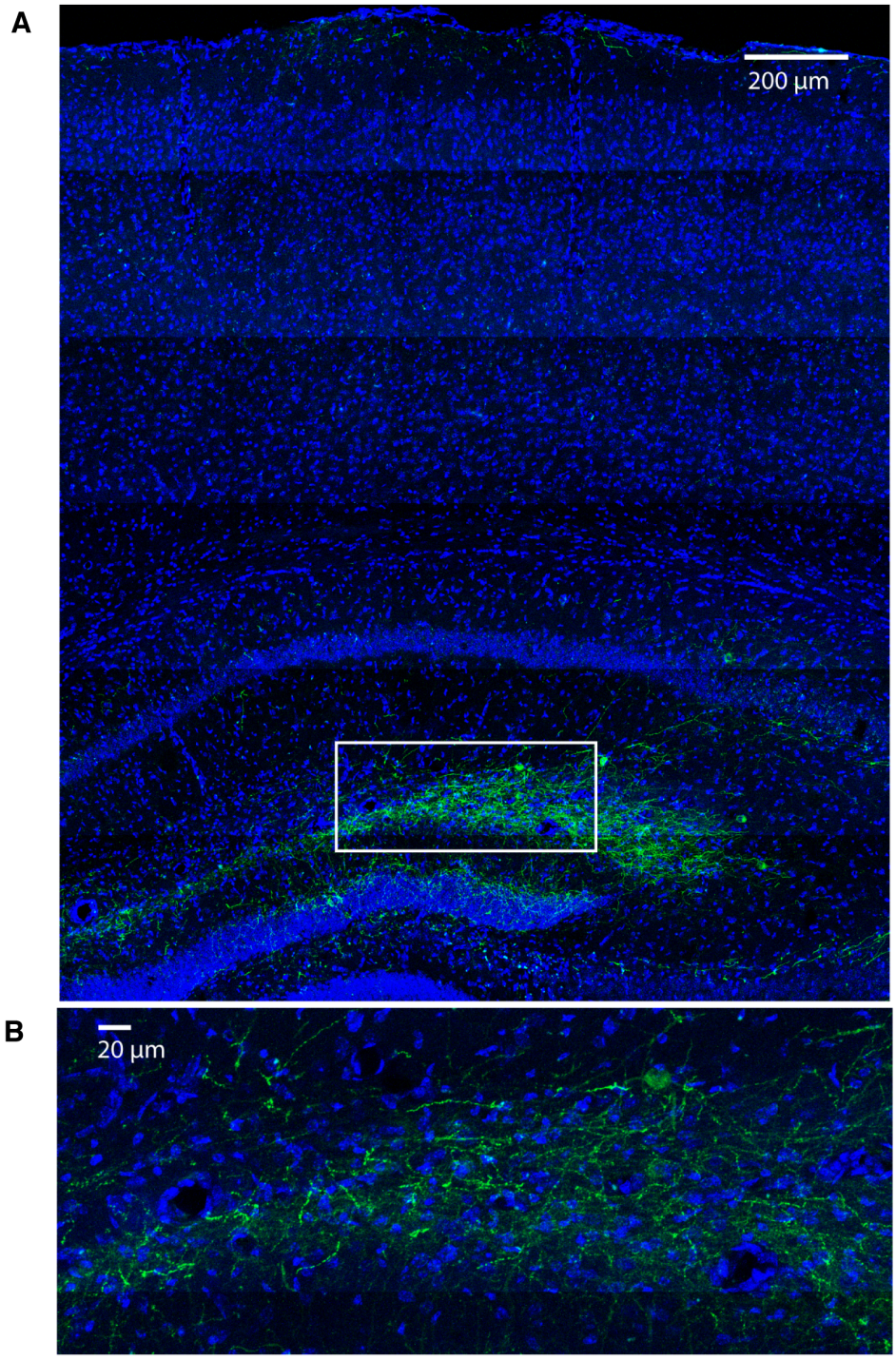

Fig S6. Hippocampal-specific targeting of LEC LRIPs. A. 20x magnification confocal image of coronal section derived from a Gad2Cre mouse injected in LEC with AAV^{Cre} expressing EGFP. Image shows expression of GFP was largely

restricted to hippocampus, with few fibers in overlying neocortex. GFP in green and DAPI in blue. **B.** Zoomed in image of area of interest indicated in A (white rectangle), showing LRIPs expressing GFP (green) in SLM/SR border of CA1 and DAPI (blue). Note: Because the LRIPs are localized to hippocampus in this brain area, our local PSEM infusion, whose extent is indicated by the mRuby fluorescence in figs. S4 and S5, will selectively target LRIPs within hippocampus.

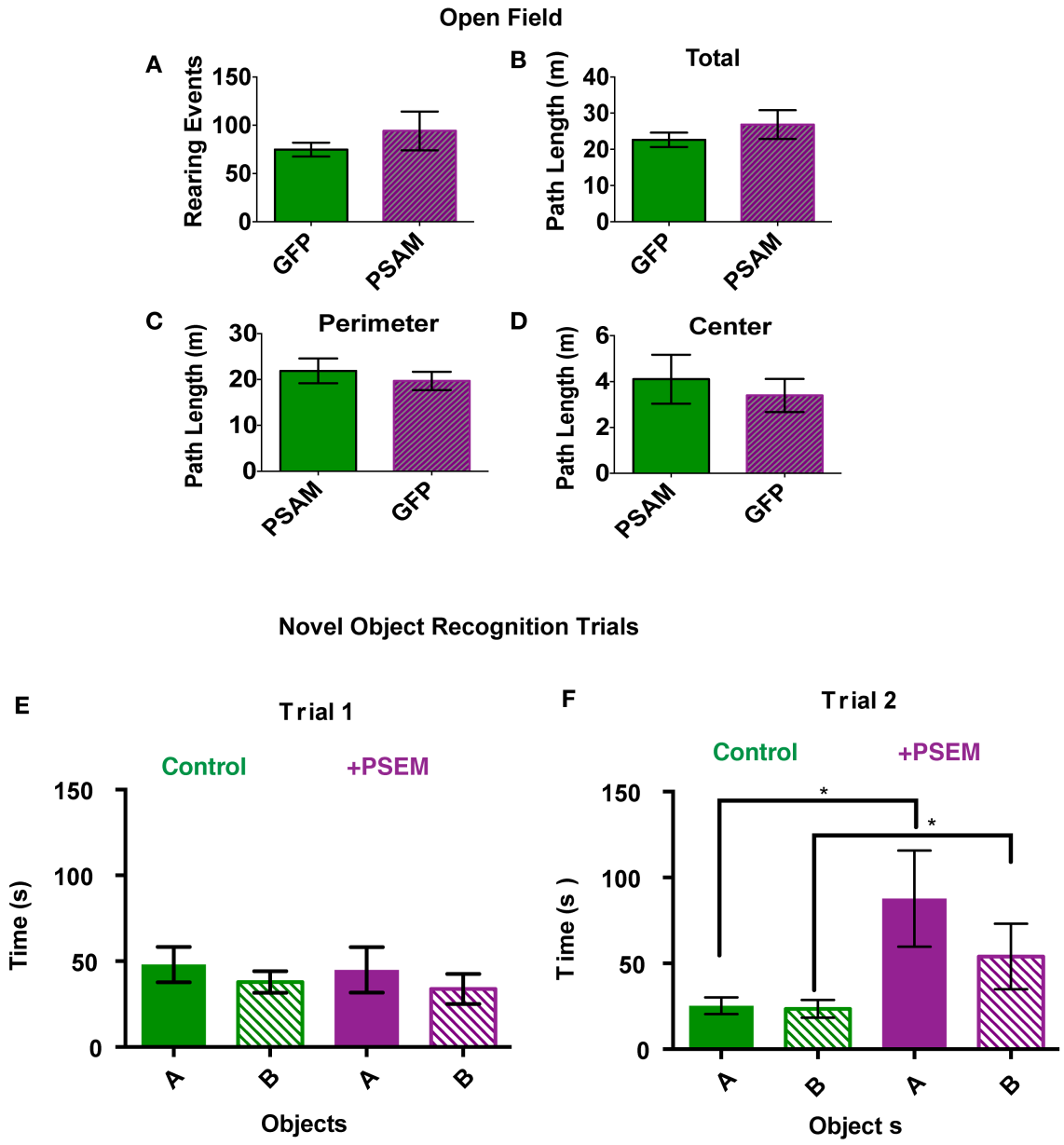
Open Field
A
Rearing Events
150
100
50
0
GFP
PSAM
B
Total
Path Length (m)
40
30
20
10
0
GFP
PSAM
C
Perimeter
Path Length (m)
30
20
10
0
PSAM
GFP
D
Center
Path Length (m)
6
4
2
0
PSAM
GFP
Novel Object Recognition Trials
E
Trial 1
Control
+PSEM
Time (s)
150
100
50
0
A
B
A
B
Objects
F
Trial 2
Control
+PSEM
*
*
Time (s)
150
100
50
0
A
B
A
B
Object s

Fig. S7. No change in anxiety or locomotor behavior in the open field test upon LEC LRIP silencing with PSEM/PSAM. **A**. Number of rearing events (±SEM) of mice in an open field 5 minutes after infusion with PSEM (0.5 μl of 15 μM solution). The mice expressed either GFP or PSAM in LEC. **B, D**. Total path length (B), portion of path length restricted to perimeter (**C**), and portion of path length restricted to the center (**D**) of open field. There was no significant difference between the control group, expressing GFP in the LRIPs, and the LRIP-silenced group, expressing PSAM ($P = 0.3426$, Distance covered; $P = 0.3557$, Rearing events). PSEM was applied to the CA1 region of both groups using a cannula. **E, F.** Bar plots of time spent with object A and B by mice in the control and PSEM groups in Trial 1 **(E)** and Trial 2 **(F)**. In trial 1, mice were exposed to object A (green circle) and object B (magenta triangle) for 10 minutes. Following a 3 minute inter-trial interval, mice were again exposed to the same pair of objects for trial 2. The mice were then tested for object recognition memory after a 10 minute interval by replacing either object A or object B with object C (orange hexagon), the novel object. Mice in which LEC LRIPs were silenced with PSEM infusion spent more time with the objects in trial 2 compared to the control group (Object A, Control, 25.30 ± 4.92 s; +PSEM, 87.7 ± 27.96 s, $P < 0.05$, t-test; Object B, Control, 23.49 ± 5.17 s; +PSEM, 53.84 ± 19.08 s; $P < 0.05$, t-test).

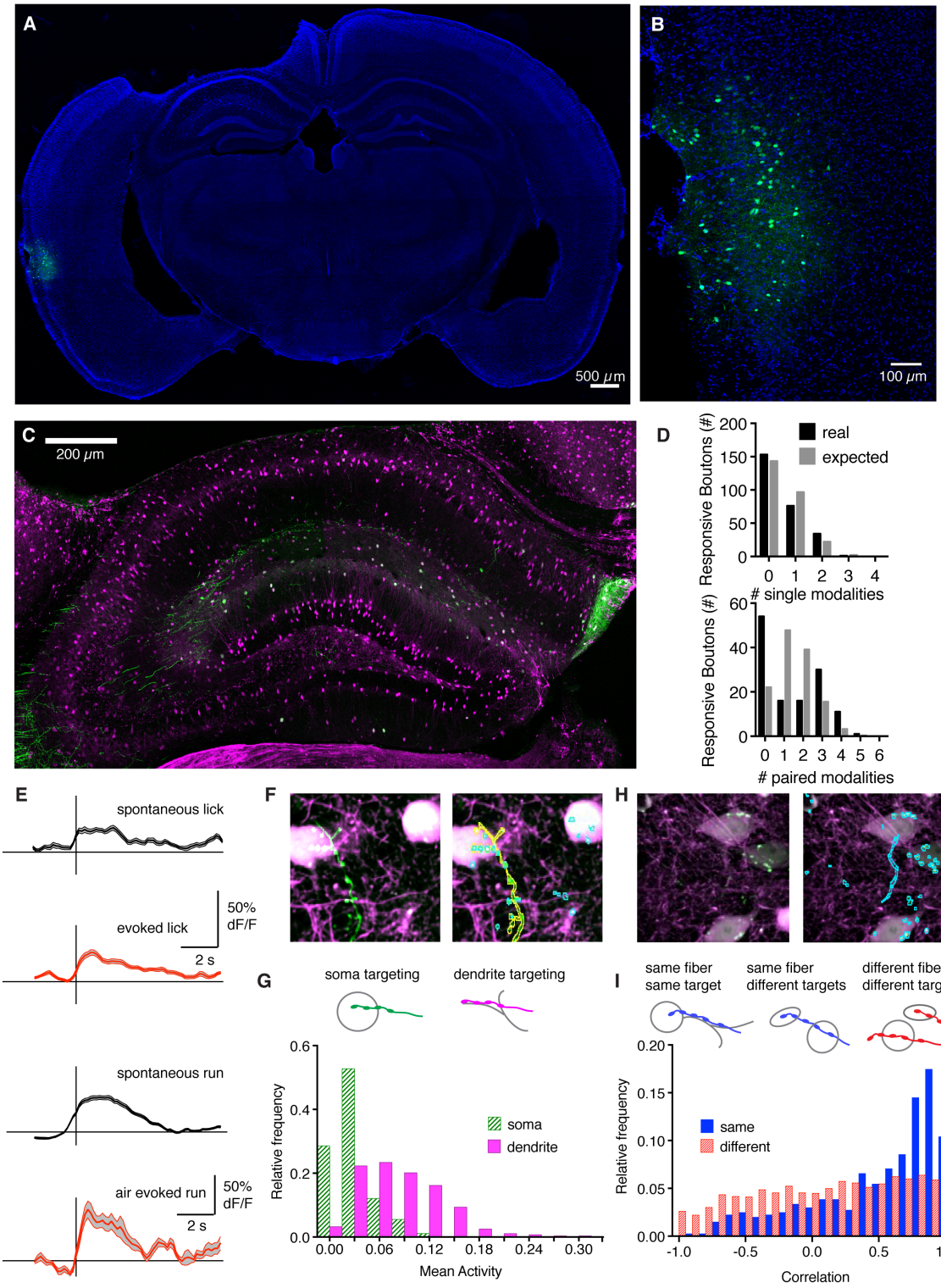
A
500 μm
B
100 μm
C
200 μm
D
real
expected
Responsive Boutons (#)
single modalities
paired modalities
E
spontaneous lick
evoked lick
50% dF/F
2 s
spontaneous run
air evoked run
F
G
soma targeting
dendrite targeting
soma
dendrite
Relative frequency
Mean Activity
H
I
same fiber same target
same fiber different targets
different fibers different targets
same
different
Correlation

Fig. S8. GCaMP6f Ca^{2+} signals in LEC LRIPs in SLM region of CA1 in response to sensory input and behavior.

A. 10X tile scan of a whole brain section, and **B.** 20X zoomed image of site of injection of AAV^{Cre} expressing GCaMP6f in LEC of left hemisphere from a GAD2-Cre mouse. $GCaMP6f^{+}$ cell bodies in green; DAPI channel in blue). **C.** 20X image of hippocampus from left hemisphere (ipsilateral to LEC injection site) showing $tdTomato^{+}$ GABAergic interneuron soma and $GCaMP6f^{+}$ LRIP axons from LEC traversing SLM of CA1. **D.** Histogram bar plots of the number of responsive boutons (Y axis) as a function of the number of stimulus modalities (X-axis) to which a given bouton responds, either with a single sensory stimulus (above) or two stimuli presented simultaneously (below). The experimental data is plotted in black while the distribution expected if the stimuli and bouton responses were independent is in gray. For single stimulus presentations, very few boutons respond to more than one type of stimulus, following the predictions for independent responses ($P = 0.01659$). In contrast, paired stimuli evoke Ca^{2+} responses in a greater than expected number of boutons ($P < 0.03$), perhaps the influence of a single overlapping stimulus in paired modalities (e.g. bouton responding to airpuff alone would likely respond to all 3 pairings with air, A+T; A+L, A+W). **E.** Average Ca^{2+} responses (± SEM) elicited by behavioral activity of licking and running. Spontaneous responses (black) include all running or licking bouts observed in the absence of a closely-timed external stimulus (airpuff, water, tone, or light). Evoked responses (red) occurred synchronously

with a particular stimulus. The rise time and peak of the ΔF/F Ca^{2+} signal is tightly time-locked to the stimulus presentation in the evoked lick and run PSTHs. **F-H.** Time-averaged images of $tdTom^+$ IN soma and dendrites and $GCaMP^+$ LRIP axons and their terminals in CA1, depicting the ROIs for LRIP boutons (cyan) and an associated axon (yellow). **F, G.** Images (**F**) and schematic drawing (**G**) showing that LRIP boutons along a single axon may target different cellular compartments of CA1 INs, such as soma versus dendrite, as well as different cells. **H, I.** Images (**H**) and schematic drawing (**I**) showing LRIP boutons from more than one axon may target the same CA1 IN. **G.** Histogram frequency plot of ΔF/F peak Ca^{2+} responses (X axis) for LRIP boutons targeting $tdTom^+$ CA1 IN dendrites (magenta, mean ΔF/F = 0.086 ± 0.004, n = 278) or soma (green, ΔF/F = 0.03 ± 0.002, n = 91; significant response difference in dendrite- versus soma-targeting boutons, $P < 0.0001$) **I.** Relative frequency distribution of bouton-bouton Ca^{2+} response correlation coefficients for all identifiable bouton pairs originating from the same axon segment (solid blue, r = 0.488 ± 0.017, n = 808) versus boutons from different axons (cross-hatched red, r = 0.115 ± 0.009, n = 3992; $P < 0.0001$, Mann-Whitney U test). Response similarity was determined by calculating the z-scored response magnitude for each stimulus for each bouton and then comparing the responses of pairs of boutons by calculating the correlation between their responses across all stimuli.

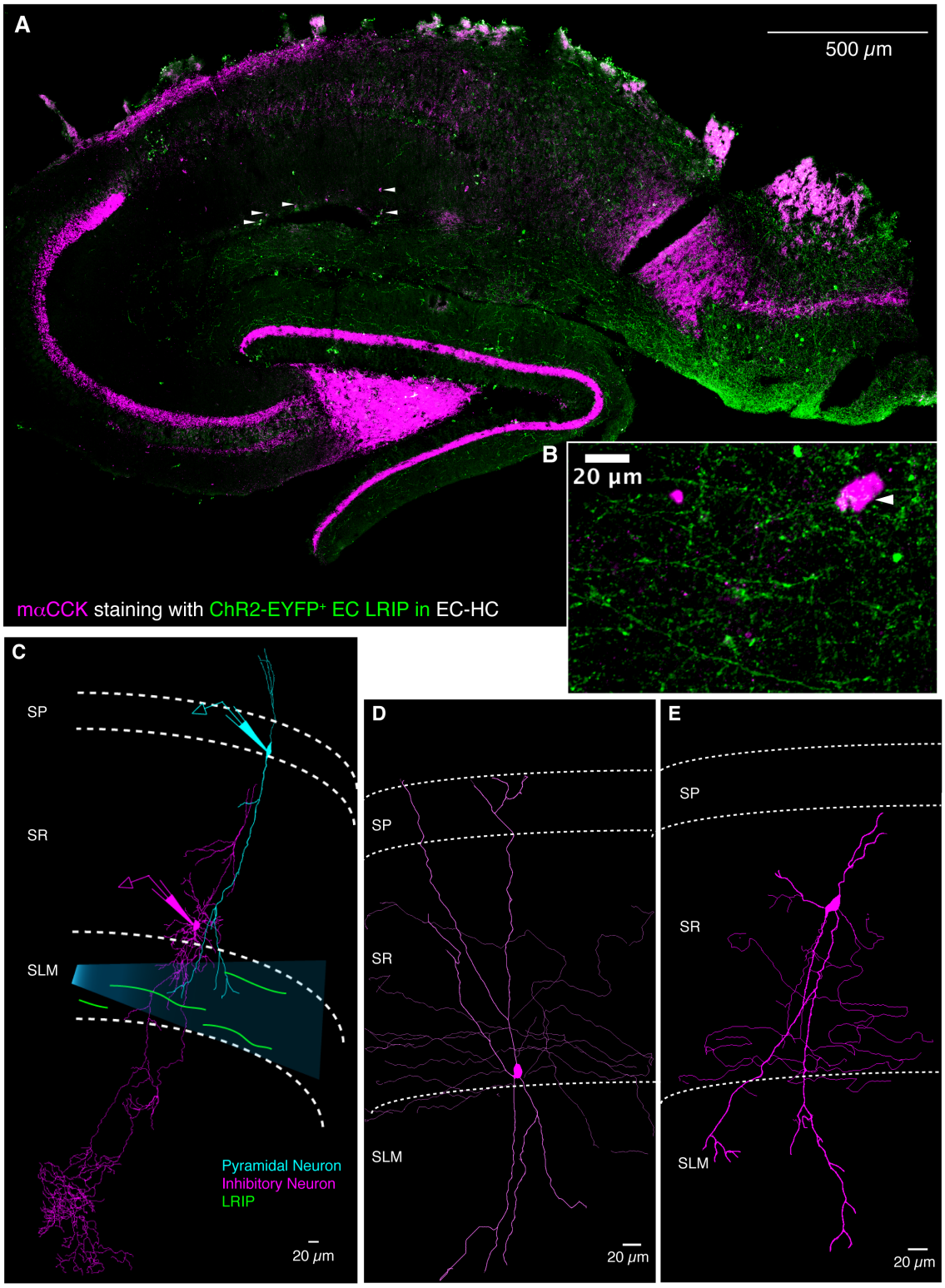
A
500 μm
mαCCK staining with ChR2-EYFP+ EC LRIP in EC-HC
B
20 μm
C
SP
SR
SLM
Pyramidal Neuron
Inhibitory Neuron
LRIP
20 μm
D
SP
SR
SLM
20 μm
E
SP
SR
SLM
20 μm

Fig. S9. Cholecystokinin-expressing (CCK) dendrite targeting interneurons are a major target of EC LRIPs in CA1. A. 20X confocal tile scan image of a transverse hippocampal section depicting ChR2-EYFP^{+} LRIP inputs from MEC and LEC (green) and anti-mouse CCK ab immunostaining (magenta). A Gad2-Cre mouse was injected with AAV^{Cre} in MEC and LEC to express ChR2 in all EC Cre^{+} GABAergic neurons. Hippocampal slices from these mice were first used for slice electrophysiology to map GABAergic connectivity between EC and CA1, followed by resectioning and immunostaining post-fixation. Mouse anti-CCK labeled IN soma in the SR/SLM border showing close proximity to LRIP axons are indicated with white arrowheads. **B.** Inset shows a 60X zoomed in image of LRIP axon terminals (white) impinging on a CCK immunopositive cell body (magenta) located in SLM of CA1. **C.** Neuronal tracing-based reconstruction of a putative CCK IN (magenta) that receives direct GABAergic and glutamatergic inputs from EC and glutamatergic inputs via SC. The CCK IN axon targets the dendrites of a dually-recorded CA1 PN (cyan). Both cells were intracellularly filled with biocytin during the recordings. The ChR2-EYFP^{+} LRIP axons traced using fluorescence guidance are shown in green. Laser light was used to photostimulate these axons and evoke an IPSC in the filled IN. This particular interneuron not only innervates the apical dendrite of the CA1 PN in SR and SLM but also sends axonal projections to DG, similar to a dendrite-targeting class of CCK INs identified *in vivo* in a previous study (*38*). **D-E.** Representative neuronal reconstructions of CA1 INs that receive LEC LRIPs, as determined by the

presence of IPSCs recorded in the IN soma in response to photostimulation of ChR2-EYFP^{+} LRIP axons. The morphology of both INs is prototypical of SC-associated CCK INs targeting CA1 PN dendrites (*23, 38, 53-57*).

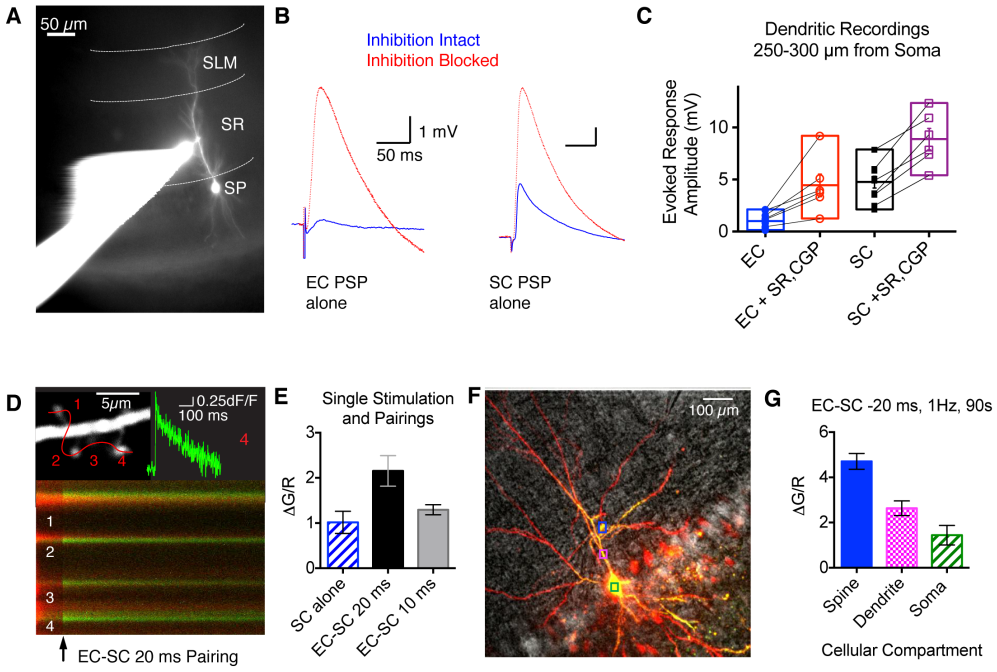

Fig. S10. CA1 PN dendritic depolarization and Ca^{2+} signaling with EC and SC stimulation. A. Representative gray scale epifluorescence image of a CA1 PN filled with Alexa Fluor 594 through an intracellular patch pipette during whole cell recording from the proximal apical dendrite (250 μm from the soma). Dendritic recordings for Fig. 6 F-H were performed at comparable locations. **B.** Whole cell voltage recordings from the proximal dendrite of a CA1 PN of PSPs elicited by electrical stimulation of EC and SC inputs with inhibition intact (blue) or blocked with SR, CGP (red). **C.** Floating bar (Mean ± SEM) and scatter plot (individual cells) of PSP amplitude in proximal dendrites of CA1 PNs with EC and SC stimulation before and after application of GABAR blockers. With inhibition intact the average EC depolarizing PSP is 1.02 ± 0.24 mV, which increased to 4.43 ± 0.11 mV with GABARs blocked ($P < 0.001$, two-tailed paired t-test, n = 6).

For SC input stimulation, average PSP amplitude was 4.75 ± 0.56 mV with inhibition intact and 8.87 ± 1.03 mV with inhibition blocked (P = 0.0011, two-tailed paired t-test, n = 6). **D.** Upper inset shows an example image of an Alexa-filled CA1 PN dendrite in stratum radiatum, showing the path for line scanning (red) of fluorescence signal in four dendritic spines (numbered 1-4). Ca^{2+} transient from one spine (green) measured from Fluo5F fluorescence change (dF/F) in response to a single EC-SC paired stimulation at a 20 ms interval (EC before SC). Lower panel shows green (Fluo-5F) and red (Alexa fluor 594) channel overlay line scans in 4 spines in response to the paired stimulation. **E.** Mean ratiometric Ca^{2+} responses (**Δ**G/R, ± SEM) recorded from proximal dendritic spines of CA1 PN upon stimulation of SC input alone (blue diagonal hatched**,** **Δ**G/R = 1.02 ± 0.25, n = 5), single paired stimulation of EC-SC inputs at a 20 ms interval (black; **Δ**G/R = 2.15 ± 0.34, n = 5) versus 10 ms (gray; **Δ**G/R 1.29 ± 0.11, n = 5) pairing intervals. The Ca2+ signal evoked by EC-SC pairing with a 20 ms interval is significantly larger than that evoked by SC stimulation alone (P < 0.001, t-test) or pairing at a 10 ms interval (P < 0.0001, t-test). **F.** Two-photon 2-D scan image (left) of a CA1 PN intracellularly filled with Alexa Fluor 594 (red) and Fluo-5F (green) showing the Ca^{2+} signal (merged in yellow) in response to a train of -20 ms paired EC-SC stimuli delivered at 1 Hz. **G.** Mean ratiometric Ca^{2+} responses (**Δ**G/R, ± SEM) recorded from proximal dendritic spines (solid blue, **Δ**G/R = 4.7 ± 0.35, n = 15), dendritic shaft (cross hatched magenta, **Δ**G/R = 2.63 ± 0.32, n = 5) and soma (diagonal hatched green, **Δ** G/R = 1.44 ± 0.43, n = 5) of CA1 PNs

immediately after a 90 s period of 1 Hz EC-SC stimulation at a -20 ms pairing interval. The color-coded scan locations are indicated in **F.**

Video S1: In vivo imaging showing activation of LRIP boutons in SLM upon presentation of water rewards. Time averaged image showing GCaMP labeled LEC LRIP boutons (green) terminating on $tdTom^+$ GABAergic interneuron cell bodies and dendrites (magenta) in SLM of CA1 (upper left). Video showing Ca^{2+} signals (principal component analysis, color calibrated white/red - high; blue low $\Delta F/F$) in the LRIP terminals of 5 trials as they get activated when the mouse receives a water reward. The presentation of the water reward is indicated (red) apposed with time synched video plots of the behavioral responses of the mouse namely, the run signal (blue) and the lick response (green) as a function of time (s) for each trial.